

Electronic Measurements in an Alternating Magnetic Field for Studying Magnetic Nanoparticle Hyperthermia: Minimizing Eddy Current Heating

Z. Boekelheide¹, Z. A. Hussein², and S. Hartzell¹

¹Department of Physics, Lafayette College, Easton, PA 18042 USA

²Department of Electrical and Computer Engineering, Lafayette College, Easton, PA 18042 USA

In magnetic nanoparticle hyperthermia therapy and research, accurate sensors are required to monitor the temperature and, potentially, other parameters such as magnetic field or mechanical stress. Conducting materials undergo eddy current heating in an alternating magnetic field (AMF), which is problematic. However, eddy current heating is strongly dependent on the size and geometry of the conducting part, thus micro- or nano-scale electronics are a promising option. This paper reports calculations and measurements of self-heating in thin wires (thermocouples) and patterned thin films (resistive thermometers) in an AMF. Thin (40 gauge) type *E* thermocouples show no significant self-heating compared with the background, while type *K* and *T* thermocouples and thicker (20 gauge) type *E*, *K*, and *T* thermocouples show significant self-heating. A thin film resistive thermometer shows no significant self-heating compared with the background when placed parallel to the field, but has significant self-heating when placed perpendicular. Thus, electronic measurements in an AMF are feasible with appropriate material properties and geometries, and are a promising possibility for future investigations in magnetic nanoparticle hyperthermia.

Index Terms—Biomagnetics, eddy currents, hyperthermia.

I. INTRODUCTION

MAGNETIC nanoparticle hyperthermia is a promising cancer treatment in which magnetic nanoparticles are injected into a tumor and then exposed to an alternating magnetic field (AMF), typically in the hundreds of kHz. Heat released in this process damages cancerous cells [1], [2]; other mechanisms such as mechanical stress from moving or rotating particles may also contribute to cell damage [3]. Heat generation can be modeled by the linear response theory for single-domain, non-interacting particles [4]; however, there are significant limitations to this theory, which need further study [5]. Also in question are the details of heat transfer at cellular length scales [6], [7]. The nature of these thermal and mechanical mechanisms necessitates further study.

To monitor the temperature and magnetic field during magnetic nanoparticle hyperthermia therapy, and for further research into nanoparticle optimization and the mechanisms behind cell death, accurate sensors are required. Often, optical rather than electronic temperature sensors are used to avoid eddy current self-heating in conducting parts in the AMF [6], [8]. However, eddy current heating is strongly dependent on the size and geometry of the conducting part, and thus micro- or nano-scale electronics are a promising possibility for exploring the behavior of nanoparticles in an AMF.

This paper explores the feasibility of using thin wires (thermocouples) and patterned thin films (resistive thermometers) in an AMF based on minimizing self-heating. Thermocouples are ubiquitous and affordable temperature sensors already in use in many laboratories. Patterned thin

film sensors are not as readily produced, but hold promise for further miniaturization of sensors and fabrication of arrays of sensors. Our results show that electronic measurements are feasible with both thin wires and patterned thin film sensors under certain conditions.

II. THERMOCOUPLES

A. Numerical Calculations

In any conducting media in an AMF, eddy currents are induced by Faraday's law, causing Joule heating. This problem can be solved analytically for symmetric situations [9]. In a magnetic material, hysteresis heating also occurs.

We model a thermocouple wire as a cylindrical wire (radius r_{\max} , height h) aligned along the direction of the uniform, applied AMF: $\vec{H} = H_0 e^{i\omega t} \hat{z}$.

Combining Faraday's law ($\nabla \times \vec{E} = -(\partial \vec{B} / \partial t)$), Ohm's law ($\vec{J}_f = \sigma \vec{E}$), and Ampere's law in matter ($\nabla \times \vec{H} = \vec{J}_f$), where in linear media $\vec{H} = (1/\mu)\vec{B}$, we obtain the diffusion equation in \vec{H}

$$\nabla^2 \vec{H} = \mu \sigma \left(\frac{\partial \vec{H}}{\partial t} \right) \quad (1)$$

for which the solution is a Bessel function J_0 with complex argument

$$\vec{H} = \text{Re} \left[H_0 \frac{J_0((-1)^{3/4} ks)}{J_0((-1)^{3/4} kr_{\max})} e^{i\omega t} \hat{z} \right] \quad (2)$$

where s is the radial coordinate in the cylindrical coordinate system and $k = \sqrt{\omega \mu \sigma}$. Applying Ampere's law, we find the free current density \vec{J}_f

$$\vec{J}_f = \text{Re} \left[k H_0 (-1)^{3/4} \frac{J_1((-1)^{3/4} ks)}{J_0((-1)^{3/4} kr_{\max})} e^{i\omega t} \right] \hat{\phi}. \quad (3)$$

The instantaneous power dissipated per unit volume by Joule heating is ρJ_f^2 ; to find the average power, we average over a

Manuscript received November 6, 2015; revised December 12, 2015; accepted January 3, 2016. Date of publication January 5, 2016; date of current version June 22, 2016. Corresponding author: Z. Boekelheide (e-mail: boekelhz@lafayette.edu).

Color versions of one or more of the figures in this paper are available online at <http://ieeexplore.ieee.org>.

Digital Object Identifier 10.1109/TMAG.2016.2515051

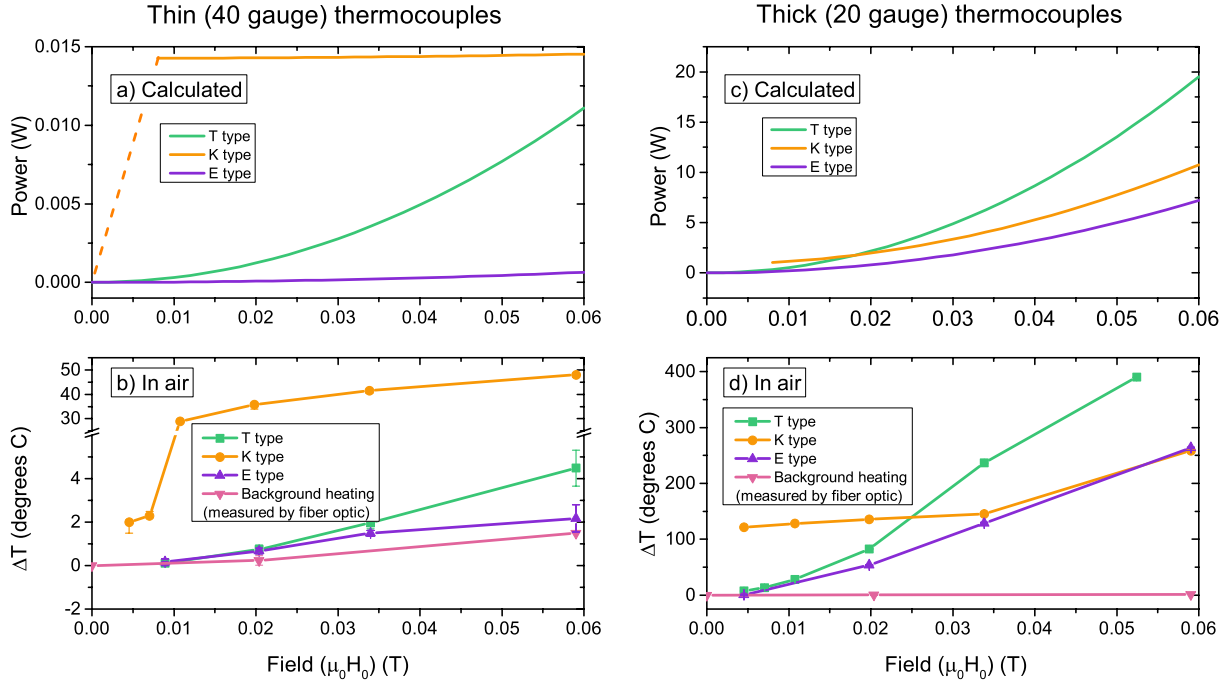


Fig. 1. Theoretical and experimental heating of thermocouples in an applied AMF, as a function of field. (a) Calculated heating power in thin (40 gauge) thermocouples. (b) Measured steady state ΔT of thin (40 gauge) thermocouples in air. (Note the break in the y-axis.) (c) Calculated heating power in thick (20 gauge) thermocouples. (d) Measured steady state ΔT of thick (20 gauge) thermocouples in air.

TABLE I
NUMERICAL PARAMETERS OF THERMOCOUPLES [12], [13]

Experimental parameters		
Height of wire	h	= 0.05 m
Frequency of AMF	$f (= \omega/2\pi)$	= 235,000 Hz
Wire radii		
20 gauge (thick):	r_{max}	= 0.0004064 m
40 gauge (thin):	r_{max}	= 3.937×10^{-5} m
Material properties		
Copper:	$\rho (= 1/\sigma)$	1.724×10^{-8} $\mu\Omega$ -cm
	$\mu_r (= \mu/\mu_0)$	1.00
Constantan:	ρ	4.89×10^{-7} $\mu\Omega$ -cm
	μ_r	1.00
Chromel:	ρ	7.06×10^{-7} $\mu\Omega$ -cm
	μ_r	1.00
Alumel:	ρ	2.94×10^{-7} $\mu\Omega$ -cm
	μ_r	$B_{sat}/(\mu_0 H_0)$ (see text)
Types of thermocouples		
T		Copper & Constantan
K		Chromel & Alumel
E		Chromel & Constantan

full cycle in time and integrate over the volume

$$\langle P_{\text{Joule}} \rangle = 2\pi h \rho f \int_{s=0}^{r_{\text{max}}} \int_{t=0}^{1/f} J_f^2 s ds dt. \quad (4)$$

The calculated power depends on the experimental parameters and material properties of the wire, given in Table I.

We numerically calculated the power dissipated in copper, constantan, chromel, and alumel. Pairs of these wires make up thermocouples of type T , K , and E . For the first three, $\mu_r = \mu/\mu_0 = 1$, so the power is proportional to H_0^2 and the resistivity $\rho = 1/\sigma$ solely determines the heating power.

Alumel is ferromagnetic, saturating around $\mu_0 H = 0.001$ T, with $B_{\text{sat}} = 0.1865$ T at room temperature [10]. To incorporate this behavior into our model, for each value of H_0 , we use

$\mu_r = B_{\text{sat}}/(\mu_0 H_0)$. Then the eddy current heating power is no longer simply proportional to H_0^2 .

In addition to eddy current heating, there is additional heating due to magnetic hysteresis in magnetic materials [11]

$$\langle P_{\text{Hysteresis}} \rangle = \left[\oint B dH \right] f [\pi r_{\text{max}}^2 h].$$

For alumel, $\oint B dH = 143$ J/m³ [10].¹ This adds a constant term to the power for fields large enough to fully saturate the whole volume of the wire.²

The power generated in type T , K , and E thermocouples was found by summing the heating power from individual wires in the combinations given in Table I. This is shown as a function of H_0 in Fig. 1(a) and (c) for two sizes of wires (40 and 20 gauge). Power is much larger in the thick wires, in which large eddy currents develop, than in the thin wires. In the thin thermocouples, type K shows the largest power due to hysteresis heating of the alumel. The hysteresis power is largely constant in H_0 and dominates because it is not size-dependent. Type T shows the next highest power, due to the high conductivity of the copper wire. Type E shows the lowest power. The three types of thick thermocouples show much more similar heating, and all follow an approximately H_0^2 profile. Type T shows the greatest heating, followed by type K , and again type E has the least heating power.

B. Experimental Results

Type T , K , and E thermocouples (Omega) of two sizes (40 and 20 gauge) were placed in an AMF supplied by

¹The sample in [10] was a toroid and our sample is a wire magnetized along the long axis; the demagnetization factor in both cases is negligible.

²For $\mu_0 H_0 \geq 0.008$ T, the full volume of the wire becomes saturated for both 20 and 40 gauge wires, so heating was only calculated for alumel at applied fields greater than this.

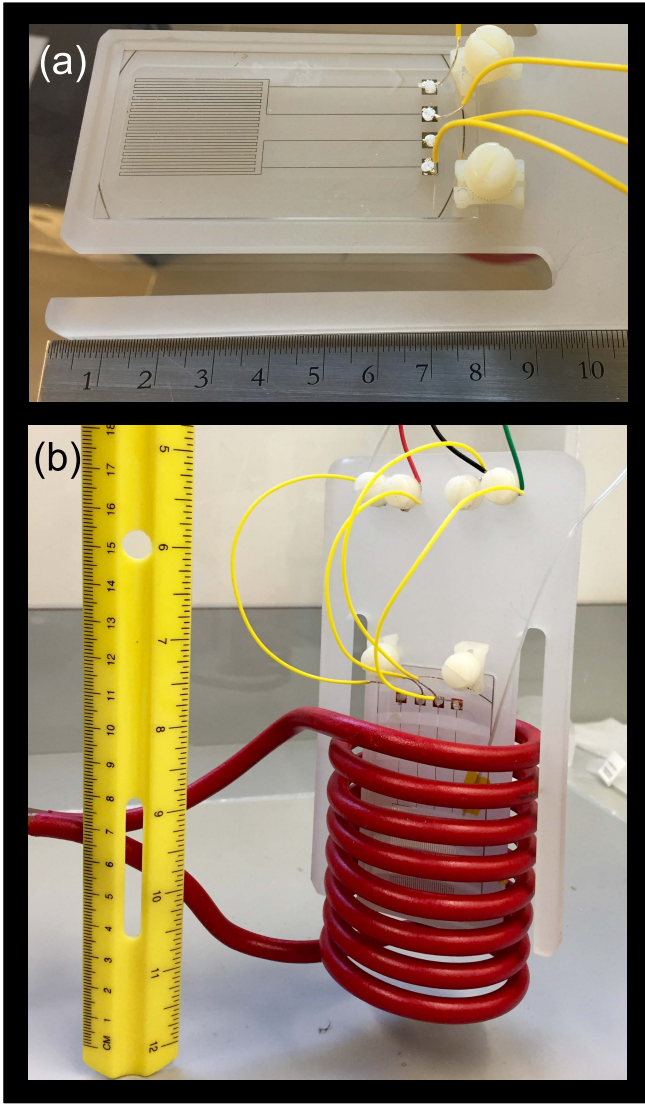


Fig. 2. (a) Resistive sensor mounted on sensor holder. (b) Resistive sensor in coil for measurement in the parallel configuration. In the perpendicular configuration, a different sensor holder is used and is inserted between two of the coil turns.

an Ambrell EasyHeat 9 kW induction heater. A home-built, water-cooled solenoidal coil was used [shown in Fig. 2(b)] at a frequency of 235 ± 5 kHz. The magnetic field was calibrated with a Fluxtrol alternating magnetic field probe such that $B_{\text{rms}} = (0.000143 \times I [\text{A}])$ T. We used $H_0 = \sqrt{2}H_{\text{rms}}$ to compare theoretical and experimental results.³ The thermocouple was inserted 0.05 m extended into the coil, parallel to the field, and the voltage was monitored with a multimeter and recorded by Labview. The coil-cooling chiller was turned ON and the temperature was allowed to stabilize, then the coil current was turned ON and the temperature was allowed to stabilize again. The steady-state temperature increase ΔT is shown as a function of H_0 in Fig. 1.

The thick (20 gauge) thermocouples all showed a large ΔT . The trends are similar to the calculated power: type *T* had the largest ΔT , followed by type *K* and type *E*. At low H_0 , type *K* had the largest ΔT , presumably due to hysteresis heating.

³The signal is not a perfect sine wave, so the rms value is a better measure of the field.

For the thin (40 gauge) thermocouples, type *K* shows the greatest ΔT , similar to the power calculation. The thin type *T* thermocouple has a very low ΔT ; although the high electrical conductivity of copper leads to a high calculated power generated by eddy currents, the high thermal conductivity of copper means that this heat is dissipated more quickly. The lowest ΔT is seen in the type *E* thermocouple.

Some of the temperature increase is due to background heating, i.e., heating from the large current passing through the coil. This background ΔT was measured with a fiber-optic temperature sensor (Opsens OTG-M170) under the same experimental conditions. The ΔT measured in the thin type *E* thermocouple is within the error of what is seen in the fiber optic sensor, suggesting that the thin type *E* thermocouple has negligible self-heating in the AMF. The ΔT measured in the thin type *T* thermocouple is slightly higher than this. This suggests that a 40 gauge type *E* thermocouple is an appropriate choice for measuring temperature in an AMF environment similar to our environment (235 000 Hz, maximum $\mu_0 H_0 = 0.059$ T) and a 40 gauge type *T* thermocouple may be appropriate for somewhat smaller f and H_0 . Furthermore, 40 gauge chromel or constantan wires could be used in other electronic measurements in such an AMF with negligible effects due to eddy currents.

Further studies of thermocouples should examine self-heating effects when the thermocouples are inserted into water, which would more closely approximate actual magnetic nanoparticle hyperthermia conditions, in which the temperature sensor is typically either inserted in a vial of liquid with nanoparticles dispersed in it during a lab experiment, or placed on living tissue to monitor the temperature during therapy.

III. PATTERNED THIN FILMS

Eddy current heating is related to the size and geometry of the conducting piece, thus microfabricated thin film sensors could have reduced heating compared to macroscopic wires. Microfabricated sensors are also advantageous because they are small and scalable, and could ultimately be incorporated into arrays of sensors, which could measure, for example, the magnetic field and temperature of an array of samples on a 2-D grid. Microfabricated thin films could also be used for other measurements, for example capacitive force sensors to study the mechanical effect of nanoparticles on cells.

We created a thin film resistive sensor, shown in Fig. 2. The film is 500 Å Au with 145 Å Cr sticking layer on a glass slide, patterned with photolithography to form a 9050 Ω meander resistor with linewidth 176 μm and four contacts for a resistance measurement.^{4,5}

The eddy currents in a well-defined loop of thin wire can be calculated from Faraday's law. The power generated by Joule heating is

$$\langle P_{\text{Joule}} \rangle = \frac{[A\mu_0 H_0 \omega \cos\theta]^2}{2R} \quad (5)$$

where R is the resistance of the loop, A is the area enclosed by the loop of wire, and θ is the angle between the applied field

⁴Using a Si wafer (10–20 Ω-cm) substrate resulted in eddy currents in the Si, leading to significant Joule heating which dominated the signal.

⁵Pt may be preferable for a resistive thermometer because of its high temperature coefficient of resistance; its higher resistance would also reduce eddy current heating. Au was used in this case because of its ease of deposition using a thermal evaporator. We may use Pt in future work.

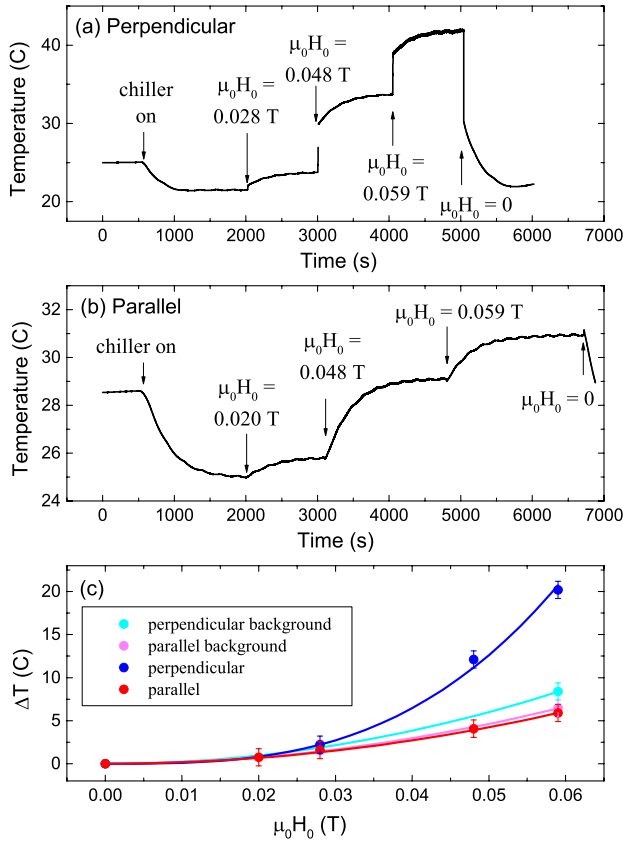


Fig. 3. Temperature versus time for resistive sensor in (a) perpendicular and (b) parallel configurations. (c) ΔT versus applied field for resistive sensor in perpendicular and parallel configurations. Lines are a guide to the eye.

and the normal vector of the area ($\theta = 0$ when the sensor is perpendicular to the field and $\theta = \pi/2$ when parallel). Thus, we expect significant heating when the sensor is perpendicular to the field, but negligible heating when parallel.

We placed our thin film sensor in the AMF in both parallel and perpendicular orientations using sample holders of non-conducting material (Fig. 2). The resistance was measured in a four-wire measurement as a function of applied field and converted into temperature using a two-point calibration of resistance versus temperature (77 K and 298 K; $dR/dT = 15.3 \Omega/^\circ\text{C}$). The temperature versus time plot is shown in Fig. 3. For each step increase of the AMF, a temperature increase ΔT is seen in both the parallel and perpendicular orientations; however, in the perpendicular orientation ΔT is larger. In addition, in the perpendicular orientation the majority of the temperature increase happens immediately, while in the parallel orientation the increase happens slowly over time (hundreds of seconds). The immediate temperature increase is most likely due to internal self-heating, while the slow increase can be attributed to the background heating.

Fig. 3(c) shows ΔT of the sensor as a function of applied field as well as ΔT due to background heating (again measured fiber optically) in both the parallel and perpendicular configurations. The background heating is different for the parallel and perpendicular configurations, because different orientations result in different heat distribution around the coil.

The ΔT measured in the thin film sensor in the perpendicular configuration is significantly larger than the

background ΔT , and, therefore, this sensor should not be used in the perpendicular configuration for thermally sensitive measurements.⁶ The ΔT measured in the parallel configuration is within error of the background ΔT and thus is promising for future measurements; however, the large background heating should be addressed by further cooling the coil and insulating the sample holder from the coil.

IV. CONCLUSION

In conclusion, thin macroscopic wires and patterned thin film sensors can be used for electronic measurements in an AMF environment. In a typical AMF used for magnetic hyperthermia, 40 gauge type *E* thermocouples display insignificant heating compared with the background heating of the coil. Patterned metallic thin films oriented parallel to the applied field also display insignificant heating. Further work miniaturizing the thin film sensors will further decrease the heating, which is promising for future electronic measurements inside the AMF environment.

ACKNOWLEDGMENT

The authors would like to thank M. Karner for making the coil and sensor holders and to the Bolton Fund for Research Experiences in Math, Biology, Physics, and Chemistry for student support.

REFERENCES

- [1] R. K. Gilchrist, R. Medal, W. D. Shorey, R. C. Hanselman, J. C. Parrott, and C. B. Taylor, "Selective inductive heating of lymph nodes," *Ann. Surgery*, vol. 146, no. 4, pp. 597–606, 1957.
- [2] A. Hervault and N. T. K. Thanh, "Magnetic nanoparticle-based therapeutic agents for thermo-chemotherapy treatment of cancer," *Nanoscale*, vol. 6, pp. 11553–11573, Aug. 2014.
- [3] L. Asín, M. R. Ibarra, A. Tres, and G. F. Goya, "Controlled cell death by magnetic hyperthermia: Effects of exposure time, field amplitude, and nanoparticle concentration," *Pharmaceutical Res.*, vol. 29, no. 5, pp. 1319–1327, May 2012.
- [4] R. E. Rosensweig, "Heating magnetic fluid with alternating magnetic field," *J. Magn. Mater.*, vol. 252, pp. 370–374, Nov. 2002.
- [5] C. L. Dennis and R. Ivkov, "Physics of heat generation using magnetic nanoparticles for hyperthermia," *Int. J. Hyperthermia*, vol. 29, no. 8, pp. 715–729, 2013.
- [6] L. Polo-Corrales and C. Rinaldi, "Monitoring iron oxide nanoparticle surface temperature in an alternating magnetic field using thermoresponsive fluorescent polymers," *J. Appl. Phys.*, vol. 111, no. 7, p. 07B334, 2012.
- [7] Y. Rabin, "Is intracellular hyperthermia superior to extracellular hyperthermia in the thermal sense?" *Int. J. Hyperthermia*, vol. 18, no. 3, pp. 194–202, 2002.
- [8] C. L. Dennis *et al.*, "Nearly complete regression of tumors via collective behavior of magnetic nanoparticles in hyperthermia," *Nanotechnology*, vol. 20, no. 29, p. 395103, Sep. 2009.
- [9] W. R. Smythe, *Static and Dynamic Electricity*, 3rd ed. Bristol, PA, USA: Hemisphere, 1989.
- [10] J. L. Horton, T. G. Kollie, and L. G. Rubin, "Measurement of *B* versus *H* of alumel from 25 to 180 °C," *J. Appl. Phys.*, vol. 48, no. 11, p. 4666, 1977.
- [11] B. D. Cullity and C. D. Graham, *Introduction to Magnetic Materials*, 2nd ed. Piscataway, NJ, USA: IEEE Press, 2009.
- [12] Omega Technical Sheet. *Physical Properties of Thermoelement Materials*. [Online]. Available: <http://www.omega.com/temperature/Z/pdf/z016.pdf>, accessed Feb. 25, 2016.
- [13] A. V. Inyushkin, K. Leicht, and P. Esquinazi, "Magnetic field dependence of the sensitivity of a type E (chromel–constantan) thermocouple," *Cryogenics*, vol. 38, no. 3, pp. 299–304, Mar. 1998.

⁶*In situ* field measurements by induced voltage would necessarily involve a loop of wire in the perpendicular configuration.